VEHICLE ACTIVITY INDICATION FROM AIRBORNE LIDAR DATA OF URBAN AREAS BY BINARY SHAPE CLASSIFICATION OF POINT SETS

W. Yao [a, *], S. Hinz[b], U. Stilla [a]
[a]Photogrammetry and Remote Sensing, Technische Universitaet Muenchen, Arcisstr.21, 80290 Munich, Germany
[b]Institute of Photogrammetry and Remote Sensing, Universität Karlsruhe (TH), 76128 Karlsruhe, Germany

KEY WORDS: Airborne LiDAR, Urban areas, Vehicle extraction, Motion indication, Shape analysis

ABSTRACT:
This paper presents a generic scheme to analyze urban traffic via vehicle motion indication from airborne laser scanning (ALS) data. The scheme comprises two main steps performed progressively — vehicle extraction and motion status classification. The step for vehicle extraction is intended to detect and delineate single vehicle instances as accurate and complete as possible, while the step for motion status classification takes advantage of shape artefacts defined for moving vehicle model, to classify the extracted vehicle point sets based on parameterized boundary features, which are sufficiently good to describe the vehicle shape. To accomplish the tasks, a hybrid strategy integrating context-guided method with 3-d segmentation based approach is applied for vehicle extraction. Then, a binary classification method using Lie group based distance is adopted to determine the vehicle motion status. However, the vehicle velocity cannot be derived at this stage due to unknown true size of vehicle. We illustrate the vehicle motion indication scheme by two examples of real data and summarize the performance by accessing the results with respect to reference data manually acquired, through which the feasibility and high potential of airborne LiDAR for urban traffic analysis are verified.

1. INTRODUCTION

Transportation represents a major segment of the economic activities of modern societies and has been keeping increase worldwide which leads to adverse impact on our environment and society, so that the increase of transport safety and efficiency, as well as the reduction of air and noise pollution are the main task to solve in the future (Rosenbaum et al., 2008). The automatic extraction, characterization and monitoring of traffic using remote sensing platforms is an emerging field of research. Approaches for vehicle detection and monitoring rely not only on airborne video but on nearly the whole range of available sensors; for instance, optical aerial and satellite sensors, infrared cameras, SAR systems and airborne LiDAR (Hinz et al., 2008). The principal argument for the utilization of such sensors is that they complement stationary data collectors such as induction loops and video cameras mounted on bridges or traffic lights, in the sense that they deliver not only local data but also observe the traffic situation over a larger region of the road network. Finally, the measurements derived from the various sensors could be fused through the assimilation of traffic flow models. The broad variety of approaches can be found, for instance, in compilations by Stilla et al., (2005) and Hinz et al., (2006).

Nowadays, airborne optical cameras are widely in use for these tasks(Reinartz et al., 2006). Yet satellite sensors have also entered into the resolution range (0.5-2m) required for vehicle extraction. Sub-metric resolution is even available for SAR data since the successful launch of TerraSAR-X. The big advantage of these sensors is the spatial coverage. Thanks to their relatively short acquisition time and long revisit period, satellite systems can mainly contribute to the collection of statistical traffic data for validating specific traffic models. Typical approaches for vehicle detection in optical satellite images are described by Jin and Davis, (2007) and Sharma et al., (2006), and in spaceborne SAR images by Meyer et al., (2006) and Runge et al., (2007). For monitoring major public events, mobile and flexible systems which are able to gather data about traffic density and average speed are desirable. Systems based on medium or large format cameras mounted on airborne platforms meet the demands of flexibility and mobility. With them, large areas can be covered (up to several km^2 per frame) while keeping the spatial resolution high enough to image sufficient detail. A variety of approaches for automatic tracking and velocity calculation from airborne cameras have been developed over the last few decades. These approaches make use of substructures of vehicles such as the roof and windscreen, for matching a wire-frame model to the image data (Zhao and Nevatia, 2003).

Despite that LiDAR has a clear edge over optical imagery in terms of operational conditions, there have been so far few works conducted in relation to traffic analysis from laser scanners. On the one hand it is an active sensor that can work day and night; on the other hand it is range senor that can capture 3d explicit description of scene and penetrate volumetric occlusions to some extent. Toth and Grejner-Brzezinska, (2006) has presented an integrated airborne system of digital camera and LiDAR for road corridor mapping and dynamical information acquisition. They addressed a comprehensive working chain for near real-time extracting vehicles motion based on fusing the images with LiDAR data. Another example of applying ALS data for traffic-related analysis can be found in Yarlagadda et al., (2008), where the vehicle category is determined by 3-d shape-based classification.

In this paper, a generic scheme to discover the vehicle motion solely from airborne LiDAR data is presented. It is based on two-step strategy, which firstly extracts single vehicles with contextual model of traffic objects and 3d-segmentation based classification (3-d object-based classification), and secondly classifies vehicle entities in view of motion status based on shape analysis.

2. VEHICLE EXTRACTION

In this step, we need to at first extract various vehicle categories as complete and accurate as possible, but not considering the difference among them in terms of dynamical status. To

* Corresponding author.

accomplish this task, we proposed a hybrid strategy that integrates context-guided progressive method with 3-d segmentation based classification. Experiments demonstrated that the assimilation of these two approaches (Fig. 1) can make our vehicle extraction from LiDAR data of urban areas more competent and robust, even against complex scenes.

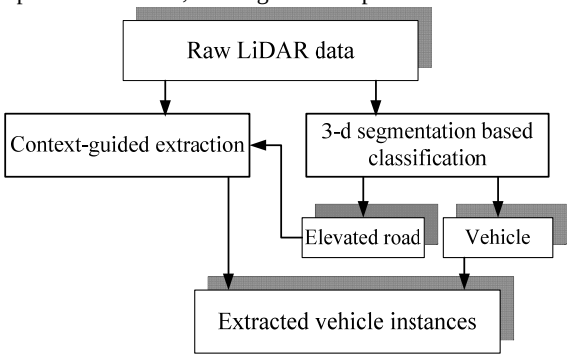

Figure 1. Integrated scheme for vehicle extraction.

2.1 Context-guided extraction

This extraction strategy comprises knowledge about how and when certain parts of the vehicle and context model of traffic related objects in urban areas are optimally exploited, thereby forming the basic control mechanism of the extraction process. In contrast to other common approaches dealing with LiDAR data analysis, it neither uses the reflected intensity for extraction nor combines multiple data sources acquired simultaneously. The philosophy is to exploit geometric information of ALS data as much as possible primarily based on such context-relation that vehicles are generally placed upon the ground surface. Moreover, the approach on the one side can be viewed as a processing strategy progressively reducing "region of interest". It is subdivided into four steps: ground level separation, geo-tiling and filling, vehicle-top detection and selection, segmentation, which are respectively elaborated in detail in Yao et al., (2008)a. An exemplary result on one co-registered dataset is shown in Fig.2.

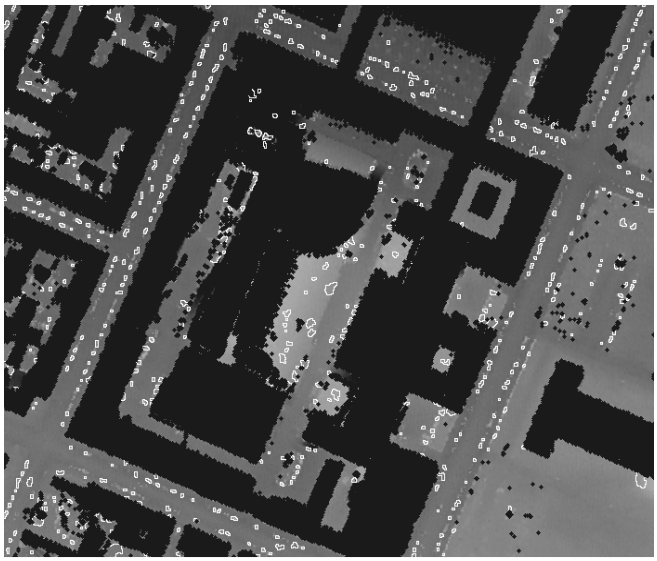

Figure 2. Vehicle extraction result as white outlined contours for test data I using context-guilded method.

2.2 3D segmentation based classification

Since many vehicles in modern cities might travel on the elevated roads such as flyover or bridge, the context relation abided by the method in section 2.1 does not always hold. Therefore, we introduced a 3D object-based classification strategy for extracting semantic objects directly from LiDAR point cloud of urban areas. It could either extract two object classes – vehicle and elevated road simultaneously or only elevated road, where vehicle can further be detected considering elevated road here as ground. The ALS data is firstly subjected to the segmentation process using nonparametric clustering tool – mean shift (MS). The obtained results are usually not able to give a significative description of distinct natural and man-made objects in complex scenes, even though MS does a genuine clustering directly on 3D point cloud to discover various geometric modes in it. Hence, the initial resulted point segments have to be handled under the global optimization criterions to generate more consistent subsets of laser data. For it, a modified normalized-cuts (Ncuts) is applied with the sense of perceptual grouping. Finally, based on derived features of spatially separated point clusters that potentially correspond to semantic object entities, classification is performed to evaluate them to extract the flyover and vehicle (Yao et al., 2009). Applying this approach to a one-path dataset yielded Fig.3.

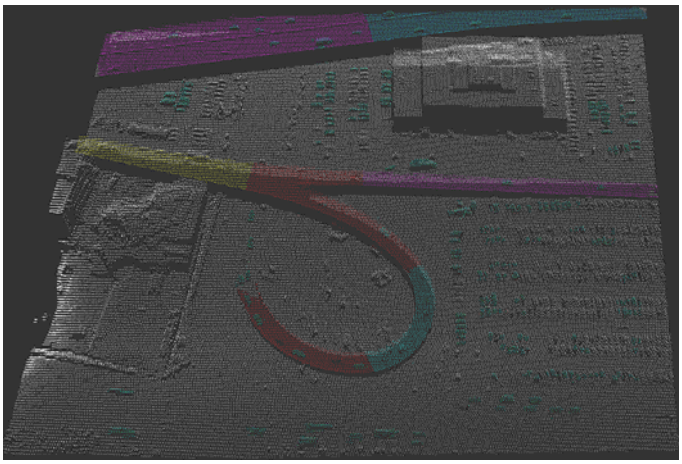

Figure 3. Vehicle (green) and flyover extraction results for test data II using 3D segentation based classification.

3. VEHICLE MOTION INDICATION

For extracted vehicles resulted from last step, the parameterized model for point sets of single vehicles can then be produced by shape analysis. From the parameterized features of vehicle shape, the across-track vehicle motion (-component) is able to be indicated unambiguously based on the moving vehicle model in ALS data, whereas the along track motion cannot be implied without prior knowledge about individual vehicle sizes. In this section, the vehicle motion status is attempted to be inferred up to the across-track direction without derive the velocity.

3.1 Vehicle Parametrization

Generally, the laser data provide us a straightforward 3D parameterization, as vehicle forms change more vertically than horizontally. To refine the 3D vehicle envelope model (Yao et al., 2008b), however, is difficult, because the laser point density acquired under common configurations is usually not sufficient to model the vertical profile of a vehicle. The situation is even more degraded by motion artifacts, because the large relative velocity of the sensor to object results in fewer laser points, making vehicle appears like a blob. Consequently, it is not easy to analytically model the vertical vehicle profiles from ALS data, which would be a simple task for much denser terrestrial laser data.

Yarlagadda et al., (2008) has applied a spoke model to vehicle database in a parking lot scanned by airborne LiDAR for 3D classification task of vehicle category. The point cloud of single vehicle is fitted with multiple connected planes being similar to spokes, which are used to describe the vehicle shape via two controlling parameters for each spoke, namely the orientation and radius of it. For the purpose of our task, it is desirable that the original vehicle form and motion artifacts are able to be captured by a unified geometric model. Due to flexibility and efficiency, the spoke model for vehicle point sets is selected here as general framework for vehicle shape parametrization. Being subject to minor modifications towards the analysis objective, the spoke model could consistently encode geometric information used for robust classification of vehicle motion.

Based on the moving vehicle model, which is focused on the 2-d deformation of vehicle form, the 3D spoke model of vehicles can be projected onto 2-d plane to deriving the shape parameters, thereby avoiding unnecessary complexities. Instead, the angle of shear and radius of projected 2-d point sets have to be estimated as controlling parameters of modified spoke model for vehicle parametrization. Due to the limited point sampling rate of ALS data, the number of spokes in the model is flexible to be determined depending on the point density or vehicle category, despite that the vehicles in our test data are frequently modeled with only one spoke.

To obtain the geometric features of extracted vehicles, the shape analysis is to be performed on the projected point sets of the spoke model. The whole procedure mainly consists of two steps: boundary tracking and parallelogram fitting.

A modified convex-hull algorithm (Jarvis, 1977) is used to determine the boundary of a set of points, namely the spoke model of extracted vehicles. The modification is to constrain the searching space of a convex hull formation to a neighborhood. The study showed that the approach can yield satisfactory results if the point distribution is consistent throughout the dataset. Such condition could be fulfilled, as only one-path ALS data are considered for moving object. The boundary tracing method for a point set B using a modified convex hull analysis starts also with a randomly selected boundary point P. Then, we use the convex hull algorithm to find the next boundary point P_k within the neighborhood of P, which is defined as rectangle with two dimensions corresponding to the point spacing in along and across-track directions of ALS data. Finally, the approach will proceed to the newly selected boundary point and repeat the step mentioned above until the point P is selected as P_k again, as depicted in the left column of Fig.4.

Since the sampling irregularity and randomness are generally assumed to be present in the LiDAR data, the traced boundary cannot be directly used as shape description for single vehicle instances, based on which the shape analysis is performed to parameterize the vehicle point sets. Consequently, a boundary regularization process aided by analytic fitting operations is to be introduced for tackling these problems. It is noticed that most vehicles have mutually parallel directions. We can find these directions from the boundary points and fit parametric lines.
The first step in regularization is to extract the points that lie on identical line segments. This is done by sequentially following the boundary points and locating positions where the slopes of two consecutive edges are significantly different. Points on these edges are grouped to one line segment. Therefore, a set of line segments $\{l_1, l_2, ..., l_n, n \geq 4\}$ from which four longest line segment $\{L_1, L_2, L_3, L_4\}$ are selected. Each of the selected line segments is modeled by equation $A_i x + B_i y + 1 = 0$. Based on the slope $M_i = -A_i / B_i$, line segments are sorted into different groups, each of which contains line segments being parallel within a given tolerance. As we know from the defined vehicle models (Yao et al., 2008b), the vehicle point sets generally appear as a parallelogram and have only two groups of line segments, i.e. vertical and horizontal.

The next step is to determine the least squares fitting to these line segments, with the constraints that the lines segments are parallel to each other within one group, namely parallelogram fitting. The solution consists of sets of parameters required to describe four line segments, which are formed as following line equations:

$$A_i x + B_i y + 1 = 0 \qquad i = 1,2,3,4;\ j = j(\mathrm{i}) = 1,2,3,\ldots m_i$$

with the condition: $\begin{matrix} M_1 = M_3 \\ M_2 = M_4 \end{matrix} \Leftrightarrow L_1\ (L_2)$ and $L_3\ (L_4)$ are opposite sides.

where m_i is the number of points on the line segment i. However, there are no specific constraints on the line segments belonging to different groups.

Once the spoke model of vehicle point sets is constructed and parameterized (Fig.4, right column), two controlling parameters can be derived, which measure the accordance of 2-d point sets to parallelogram (non-rectangularity) and dimension scale, respectively. The angle of shear θ_{SA} of parameterized vehicle point set:

$$\theta_{SA} = \arctan\left(\left|\frac{M_2 - M_1}{1 + M_1 \cdot M_2}\right|\right),$$

The extent E of parameterized vehicle point set:

$$E = |L_1| \cdot |L_2| \cdot \sin\theta_{SA}$$

where M_2, M_1 are slopes of line segments belonging to two groups respectively and $|\ |$ indicates the length of corresponding line segment.

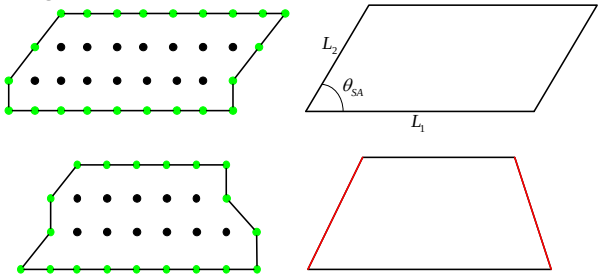

Figure 4. Two examples for vehicle parametrization: boundary tracing, shape regulation (parallelogram fitting). Top row: moving vehicle; bottom row: vehicle of ambiguous movement with abnormal laser reflections. Green points marks the borders of extracted vehicle, red lines indicate the non-parallel sides of a fitted vehicle shape.

Two basic cases have to be distinguished in view of vehicle movement, based on the geometric features derived above for each extracted vehicle. However, they occasionally emerge

other than as parallelogram (Fig.4, bottom row), but e.g. trapezoid, common quadrilaterals, etc, due to unstable sampling characteristics of LiDAR or clutter objects in urban areas. It is difficult to decide whether it is actually a moving vehicle part or a point set of stationary vehicle with missing parts. Generally, these vehicle point sets confuse the shape analysis and deliverer only ambiguous geometric features that cannot be adopted for robust classification. Therefore, this category of vehicle point sets have to be identified and then excluded from candidates delivered to movement classification, which means that they could be only attributed to uncertain motion status at the moment. Those point sets are also undergone the same shape analysis process and can be found when the parallelogram fitting fails.

3.2 Movement classification

As indicated in section 3.1, the point sets of extracted vehicle can generally be denoted by spoke model with two parameters, whose configuration is formulated as

$$X = \begin{pmatrix} U_1 \\ . \\ . \\ U_k \end{pmatrix}, \quad U_i = \begin{pmatrix} \theta_{SA}^i \\ E_i \end{pmatrix}$$

where k denotes the number of spokes in the model. As inspired by the works of Fletcher et al., (2003) and Yarlagadda et al., (2008), the 3D vehicle shape variability is nonlinear and represented as a transformation space. Thus the similarity between vehicle instances can be measured by group distance metric. It has been also confirmed that Lie group PCA can better describe the variability of data that is inherently nonlinear and statistics on linear models may benefit from the addition of nonlinear information. Since our task is intended to classify the vehicle motion based on the shape features of vehicle point sets, the classification framework for distinguishing generic vehicle category can be easily adapted to motion analysis.

Consequently, a new vehicle configuration Y can be obtained by a transformation of X written in matrix form: $Y=T(X)$ where

$$T = \begin{pmatrix} M_1 & . & 0 \\ . & . & . \\ 0 & . & M_k \end{pmatrix}, \quad M_i = \begin{pmatrix} R_i & 0 \\ 0 & e^{ai} \end{pmatrix}$$

, R_i denotes the 2-d rotation acting on the angle of shear θ_{SA} . e^{ai} denotes the scale acting on the extent E. By varying T, different vehicle shape (motion status) can be represented as transformations of X. based on elaborations in Rossmann (2002), M_i is a Cartesian product of the scale and angle value groups $\Re \times \mathbf{SO}(2)$, which are the Lie group of 1-d real value and the Lie group of 2-d rotation, respectively. Since the Cartesian product of Lie group elements is a Lie group and T is the Cartesian product of transformation matrices M acting on the individual spokes, T forms a Lie group. The group T is a transformation group that acts on shape parameters M. However, any vehicle shape X may be represented in T as the transformation of a fixed identity atom.

A group is defined as a set of elements together with a binary operation (multiplication) satisfying the closure, associative, identity and the inverse axioms. A Lie group G is a group defined on differentiable manifold. The tangent space of group G at the identity e, T_e , is called the Lie algebra g. The exponential map *exp* is a mapping from Lie algebra elements to Lie group elements. The inverse of the exponential map is called logarithmic map *log*. The Lie algebra element of T is obtained by performing component-wise log operation on each of the M_i :

$$\log(T) = \begin{pmatrix} \log(M_1) & . & 0 \\ . & . & . \\ 0 & . & \log(M_k) \end{pmatrix} \qquad (1)$$

where $\log(M_i) = \alpha_i \begin{pmatrix} 1 & 0 \\ 0 & 1 \end{pmatrix} + \theta_i \begin{pmatrix} 0 & -1 \\ 1 & 0 \end{pmatrix}$. Equation (1) expresses the Lie algebra element of an individual spoke in terms of the generator matrices for scaling and 2-d rotation factors.

The intrinsic mean μ of a set of transformation matrices T_1 , T_2 , …, T_n of vehicle spoke models is defined as

$$\mu = \arg\min \sum_{k=1}^{n} d(T_1, T_2)^2 \qquad (2)$$

where $d(\cdot,\cdot)$ denotes Riemannian distance on G, and $d(T_1,T_2) = \left\| \log(T_1^{-1}T_2) \right\|$ where $\|\cdot\|$ is the Frobenius norm of the resulting algebra elements. The 1-parameter Lie algebra element of the spoke model of vehicle point sets is given by

$$A_v(t) = \begin{pmatrix} A_{v_1}(t) & . & 0 \\ . & . & . \\ 0 & . & A_{v_n}(t) \end{pmatrix} \qquad (3)$$

where $A_{v_i}(t) = t\log(M_i)$, denoting that the Lie algebra element is defined at a fixed (α_i, θ_i) for each spoke, which represents the tangent to a geodesic curve parameterized by t. The parameter t in (3) sweeps out a 1-parameter sub-group, $H_v(t)$ of the Lie group G of spoke transformations. For any $g \in G$, the distance between g and $H_v(t)$ is defined as

$$d(g, H_v) = \min d(g, \exp[A_v(t)]), \quad t \in \Re \qquad (4)$$

Analogous to the principle components of a vector space, there exist 1-parameter subgroups called the principle geodesic curves (Fletcher et al., 2003) which describe the essential variability of the data points lying on the manifold. The first principle geodesic curve for elements of a Lie group G is defined as the 1-parameter subgroup $H_{v^{(1)}}(t)$, where

$$v^{(1)} = \arg\min \sum_{i=1}^{n} d^2(\mu^{-1}g_i, H_v) \qquad (5)$$

Let $p_{i,1}$ be the projection of $\mu^{-1}g_i$ on $H_{v^{(1)}}$, and define $g_i^{(1)} = p_{i,1}^{-1}\mu^{-1}g_i$. The higher k-th principle geodesic curve can be determined recursively based on (5).

The motion analysis can then be formulated as a binary classification problem using Lie distance metrics. The input to the Lie distance classifier comprises a set of labeled samples T_j from two categories of vehicle status C_j - moving vehicles and stationary ones. n_Y denotes the number of training samples for each category. The intrinsic mean μ_j and the principal geodesics $H_{v^{(n)}}$ are computed for each vehicle class C_j using

the samples $S_j^m \in S_j$, $1 \le m \le n_Y$. Once the principal geodesics are available for each C_j, the classification of an unlabeled sample x can be performed by finding the category with the closest first principal geodesics to x. The corresponding motion status of a vehicle is found by

$$j^* = \arg\min \left\| \log(H_{j,v^{(1)}}^{-1} x) \right\|, \quad j \in \{1,2\} \qquad (6)$$

Generally, it is claimed that the classification of vehicle status can successfully run based solely on the first principal geodesics of a movement category. Although there are significant variations in shape over one category, the first principal geodesics $H_{v^{(1)}}$ is assumed to summarize the essential shape features of vehicle point sets in terms of only distinguishing between binary motion statuses.

3.3 Results

We used the same vehicle datasets as derived in the section 2 to assess the proposed algorithm intended for classifying the motion status. Both of datasets are acquired over $300 \times 400\ m^2$ dense urban areas with averaged point density of about 1.4 pts/ m^2. The only one difference between them is that the first one used is co-registered from multiple strips rather than one-path. The classification results of vehicle motion status are presented in Fig.5. To access the performance of Lie group based classifier, minimum distance classifier was used to classify the same datasets based on the feature space spanned by vehicle parametrization.

The test dataset each consists of more than 50 vehicles successfully detected by vehicle extraction process. A set of 5 vehicle samples from each motion category is manually selected to train the classifier for vehicle motion status at first. It can be expected that poorly chosen training samples due to the strong shape variability in the category of moving vehicle could have a negative effect on classification performance. Therefore, the selection of training data for moving vehicle category should be carried out in such way that the fundamental shape information are expressed and generalized. Receiver Operating Characteristic (ROC) curves are generated by comparing classification results with reference data manually acquired by human interpretation and shown in Fig.6 for respective test datasets.

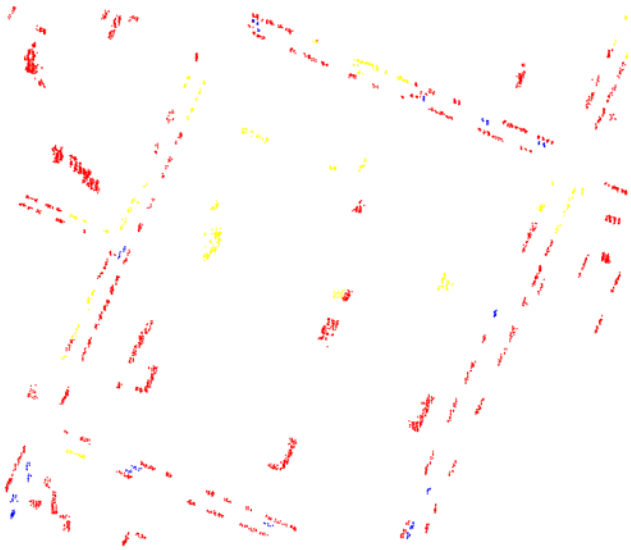

(a)

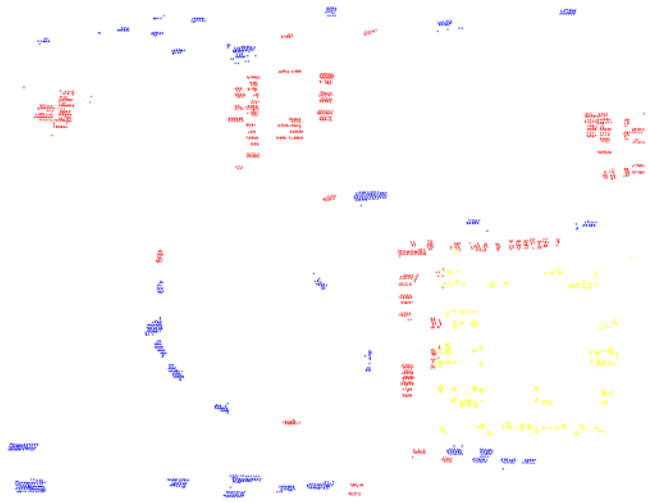

(b)

Figure 5. Vehicles motion classification results for dataset I and II (top-view of vehicle point sets). Blue: moving; Red: stationary; Yellow: uncertain.

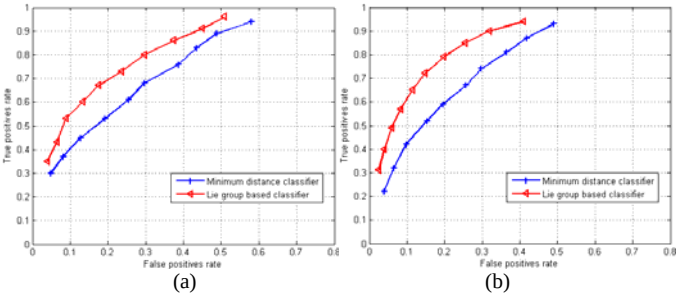

(a) (b)

Figure 6. ROC curves for vehicle motion classification. (a) Dataset I; (b) Dataset II.

3.4 Discussion

Since we do not have real "ground truth" for vehicle motion which could be simultaneously captured along the scanning campaigns by an imaging sensor as described in Toth and Grejner-Brzezinska, (2006), the results are firstly assessed with respect to human examination abilities. Based on the context relations the vehicle movement could be roughly distinguished between moving vehicles and stationary ones. Note that the along-track motion cannot be resolved on principle if the true length is unknown, our evaluation are inherently biased by ambiguities introduced by the incorrect vehicle length.

It can be found out from the results displayed above that most of detected moving vehicles appear in the heavily travelled roads such as flyovers and main streets of city and the vehicles classified as motionless are mostly found in the parking lots or along road margins. The yellow class indicates the vehicles of uncertain status which are all nearly placed very close to each other in a parking lot and are excluded from the motion classification step due to the shape irregularity. False alarms from motion classification by our approach usually appear for slowly moving vehicles which travelled not perpendicular to the flight direction or those moving ones that are shaped by anomaly sample points in ALS data due to vegetation occlusion or unstable reflection properties. As indicated in ROC curves, the Lie group based classifier outperforms the minimum distance classifier in both cases, as its ability to generalize various shapes from training data, even for worst-cases, is demonstrated. It can also be observed that the second test

dataset generally has better performance than the first one in terms of vehicle motion classification, which has shown that one-path LiDAR data could be more appropriate for our task than co-registered data of multiple strips, despite that the point density of combined dataset would be higher. Moreover, the superior performance may trace back to the applied extraction strategy of direct 3D segmentation on LiDAR point clouds other than 2D analysis approach.

Once the motion status of extracted vehicles is determined, the velocity of moving vehicles can be inferred under the precondition that the true vehicle size is known. According to results presented here, it is easy to empirically give such performance summery that the vehicle motion indication as well as estimation from ALS data would fairly depend on certain factors, such as point density, distribution spacing between every two vehicles, relative motion direction to the flight direction, absolute velocity of vehicle, and vehicle size. The accurate impacts of single factors on motion analysis results have to be further obtained by quantitative analysis with great amount of test data

Traffic analysis could quite benefit from some distinctive operational conditions of LiDAR sensor, in comparison to optical camera. It is an active sensor less weather dependent; for example, it can cope with haze, fog and volume-scattering objects to some extent, working night too. Furthermore, scene complexity poses an additional difficulty for the optical imagery: dense urban areas, long and strong shadows, occlusions, etc., can severely impair the vehicle extraction performance.

4. CONCLUSION

Overall, a progressive scheme consisting of the vehicle extraction step followed by motion status classification is presented in this work attempting to automatically characterize the traffic scenario in urban areas. Based on single vehicle instances extracted by an approach combining context exploitation with 3D segmentation, the binary motion status of them is determined by shape analysis and classification. As indicted by the results derived from real ALS data commonly used for city mapping and modeling, traffic analysis by airborne LiDAR offers great potential to support the short/mid-term acquisition of statistical traffic data for a given road network in urban areas in despite of higher false alarm rates. Nevertheless, numerous potential improvements of the schemes have to be developed in future, in order to deal with main obstacles to LiDAR traffic characterization, especially regarding velocity estimation, such as low point density, unknown vehicle size and unstable laser reflection properties of vehicle surface.

REFERENCES

Fletcher, P.T., Conglin, L. and Joshi, S., 2003. Statistics of shape via principal geodesic analysis on Lie groups, Computer Vision and Pattern Recognition, 2003. Proceedings. 2003 IEEE Computer Society Conference on, pp. I-95-I-101 vol.1.

Hinz, S., Bamler, R. and Stilla, U. (Editors), 2006. Theme issue "Airborne and spaceborne traffic monitoring". ISPRS Journal of Photogrammetry and Remote Sensing, 61(3/4), 135-278 pp.

Hinz, S., Lenhart, D. and Leitloff, J., 2008. Traffic extraction and characterisation from optical remote sensing data. The Photogrammetric Record, 23(124): 424-440.

Jarvis, R.A., 1977. Computing the shape hull of points in the plane, IEEE Computing Society Conference on Pattern Recognition and Image Processing, New York, pp. 231–241.

Jin, X. and Davis, C.H., 2007. Vehicle detection from high-resolution satellite imagery using morphological shared-weight neural networks. Image and Vision Computing, 25(9): 1422-1431.

Meyer, F., Hinz, S., Laika, A., Weihing, D. and Bamler, R., 2006. Performance analysis of the TerraSAR-X Traffic monitoring concept. ISPRS Journal of Photogrammetry and Remote Sensing, 61(3-4): 225-242.

Reinartz, P., Lachaise, M., Schmeer, E., Krauss, T. and Runge, H., 2006. Traffic monitoring with serial images from airborne cameras. ISPRS Journal of Photogrammetry and Remote Sensing, 61(3-4): 149-158.

Rosenbaum, D., Kurz, F., Thomas, U., Suri, S. and Reinartz, P., 2008. Towards automatic near real-time traffic monitoring with an airborne wide angle camera system. European Transport Research Review.

Rossmann, W., 2002. 'Lie Groups: An introduction through linear groups. Oxford University Press.

Runge, H. et al., 2007. Space borne SAR traffic monitoring, Proceedings, International Radar Symposium, Cologne, pp. 5.

Sharma, G., Merry, C.J., Goel, P. and McCord, M., 2006. Vehicle detection in 1-m resolution satellite and airborne imagery. International Journal of Remote Sensing, 27(4): 779 - 797.

Stilla, U., Rottensteiner, F. and Hinz, S. (Editors), 2005. Object extraction for 3D city models, road databases, and traffic monitoring— concepts, algorithms, and evaluation (CMRT05) International Archives of Photogrammetry, Remote Sensing and Spatial Information Sciences, 36(3/W24), 196 pp.

Toth, C.K. and Grejner-Brzezinska, D., 2006. Extracting dynamic spatial data from airborne imaging sensors to support traffic flow estimation. ISPRS Journal of Photogrammetry and Remote Sensing, 61(3-4): 137-148.

Yao, W., Hinz, S. and Stilla, U., 2008a. Automatic vehicle extraction from airborne LiDAR data of urban areas using morphological reconstruction, Proceedings of 5th IAPR Workshop on Pattern Recognition in Remote Sensing (PRRS08), Tampa, USA, pp. 1-4.

Yao, W., Hinz, S. and Stilla, U., 2008b. Traffic monitoring from airborne LIDAR – Feasibility, simulation and analysis, XXI Congress, Proceedings. International Archives of Photogrammetry, Remote Sensing and Spatial Geoinformation Sciences, Beijing, China, pp. Vol 37(B3B):593-598.

Yao, W., Hinz, S. and Stilla, U., 2009. Object extraction based on 3d-segmentation of LiDAR data by combining mean shift and normalized cuts: two examples from urban areas, 2009 Urban Remote Sensing Joint event: URBAN 2009 - URS 2009.

Yarlagadda, P., Ozcanli, O. and Mundy, J., 2008. Lie group distance based generic 3-d vehicle classification, Pattern Recognition, 2008. ICPR 2008. 19th International Conference on, pp. 1-4.

Zhao, T. and Nevatia, R., 2003. Car detection in low resolution aerial images. Image and Vision Computing, 21(8): 693-703.